

# ON THE IDENTIFICATION OF THE SPEED POLAR DURING NORMAL SOARING FLIGHT

by Jörg F. Wagner, Stuttgart University, Germany

Presented at the XXIII OSTIV Congress, Borlänge, Sweden (1993)

## 1. Introduction – The Speed Polar

One important aid for sailplane pilots planning their flights is the speed polar ([1],[2]). Despite very detailed methods of calculation ([3],[4]), up to now one can only determine rather exactly such curves by experiments. But the classical ways for this task require special flight tests with a lot of time ([5],[6]); so one can only measure few gliders. In addition, the results have inaccuracies, which vary with time as well. Therefore a new method ascertaining the speed polar is desirable which can be simply applied and can be permanently used aboard many sailplanes. The following three sections of this paper contain basic ideas for this aim.

### 1.1 Basic Relations

The speed polar make statements about large motions

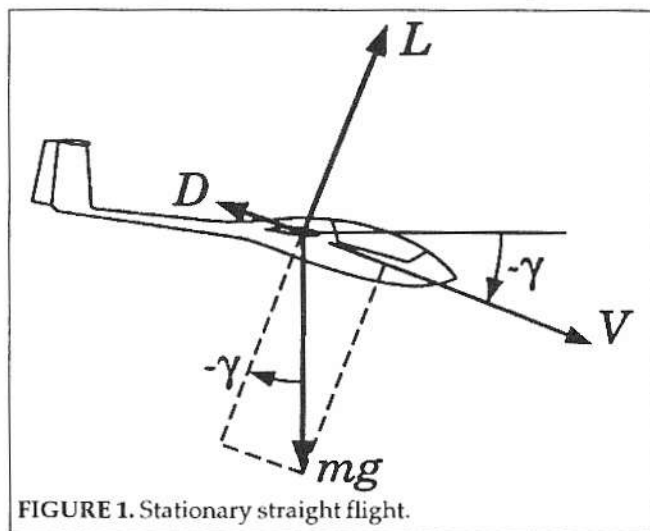


FIGURE 1. Stationary straight flight.

of the glider; so we can assume the plane being a point or a lumped mass. Additionally we neglect the wind and the density gradient of the air. With these premises the polar represents the stationary, straight flight.

Figure 1 shows the air speed  $V$  and the flight-path inclination angle  $\gamma$  of the sailplane. In the polar diagram (Figure 2), whereby both axes must have the same scale;  $u_g$  and  $w_g$  are the components of the air speed vector relative to a normal earth-fixed axis system:

$$u_g = V \cos \gamma, \quad w_g = -V \sin \gamma. \quad (1)$$

For the abscissa one uses often  $V$  instead of  $u_g$ , because  $w_g$  is usually so small that  $V \approx u_g$  (1). But here we will employ the more systematic  $u_g w_g$ -representation.

Figure 2 shows also two important optima: the path angle  $\gamma_{opt}$  of the best lift-drag ratio and the minimal sink rate  $w_{opt}$ .

During stationary, straight flight the total lift  $L$  and drag  $D$  balance the weight  $mg$  (Figure 1); using the air density  $\rho$ , the wing area  $S$ , and the aerodynamic coefficients  $C_L$ ,  $C_D$  for lift and drag we can describe this fact by two equations:

$$mg \cos \gamma = \frac{\rho V^2}{2} S C_L, \quad -mg \sin \gamma = \frac{\rho V^2}{2} S C_D \quad (2)$$

Rearrangements of the relations (1) and (2) result in expressions for  $u_g$  and  $w_g$

$$u_g = \sqrt{\frac{2mg}{\rho S}} \frac{c_L(\alpha)}{(c_L^2(\alpha) + c_D^2(\alpha))^{3/4}}, \quad w_g = \sqrt{\frac{2mg}{\rho S}} \frac{c_D(\alpha)}{(c_L^2(\alpha) + c_D^2(\alpha))^{3/4}} \quad (3)$$

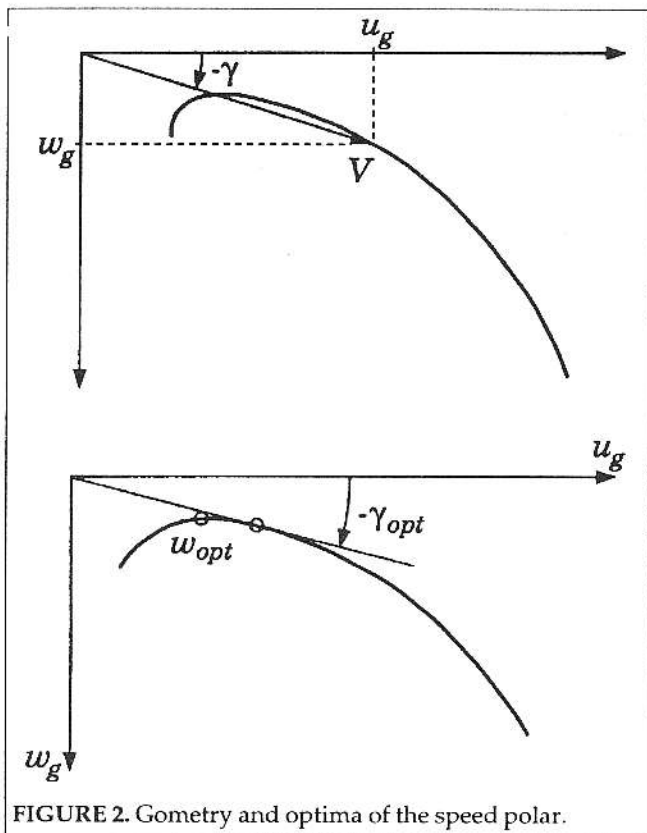


FIGURE 2. Geometry and optima of the speed polar.

This is a parametric representation of the polar, because  $C_L$  and  $C_D$  are functions of the parameter angle of attack  $\alpha$ . The last two equations facilitate the discussion of the factors which determine the speed polar:

1. The factor

$$\sqrt{2mg/\rho S}$$

shows the influence of weight and air density. These two values are not constant; therefore the polar undergoes a time dependent scaling. But we can solve this problem quite simply if we standardize the two equations with the common square root:

$$u_g^* = u_g / \sqrt{2mg/\rho S}, \quad w_g^* = w_g / \sqrt{2mg/\rho S}$$

so that the variations disappear. If one knows  $u_g^*$  and  $w_g^*$  as well as  $mg$ ,  $\rho$  and  $S$ , it is easy to calculate  $u_g$  and  $w_g$ .

2.  $u_g^*$  and  $w_g^*$  of the standardized polar are only functions of  $C_L$  and  $C_D$ . These aerodynamic parameters depend on the **sailplane type** and additionally on the **constructional details** of each individual glider as well as on the time varying **center of gravity** and **surface dirtiness**. The aim of this paper is to describe an appropriate way for the polar determination which can consider all these influence factors.

3. Finally, because the standardized polar only depends on aerodynamics, it represents merely the glider motion relative to the air. In the following  $V$  is only just the

speed relative to the air,  $V_K$  denotes the absolute flight-path velocity, and  $V_W$  stands for the wind velocity; they form the following vectorial equation:

$$\vec{V}_K = \vec{V} + \vec{V}_W \quad (4)$$

Figure 3 ([7]) shows this relation and its effect on the polar. Up to now we considered the curve of the  $V$ -motion (relative to the air), which is independent from the wind shift and is therefore fixed relative to the  $u_g w_g$ -axes; but the pilot is specially interested in the polar that results from the absolute velocity  $V_K$  ( $u_{Kg} w_{Kg}$ -axes), as the variometer indicates  $w_{Kg}$  while  $u_{Kg}$  is the ground speed. The wind variation with time has the effect that the curve moves around in the  $u_{Kg} w_{Kg}$ -diagram together with the  $u_g w_g$ -axes; this fact makes considerable difficulties for the experimental determination of the polar. In addition, the dashed lines demonstrate the clear change of the best flight-path inclination angle.

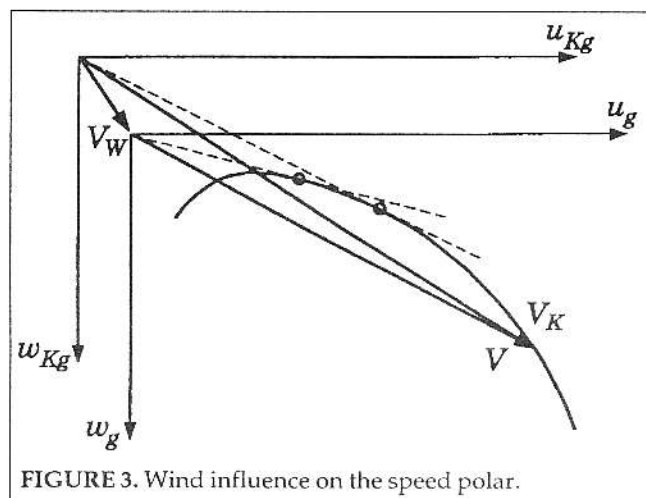


FIGURE 3. Wind influence on the speed polar.

## 1.2 Methods Determining the Speed Polar

Only the  $u_g w_g$ -diagram provides a definite polar. Determining this curve one must ascertain the glider motion relative to the air. The classical ways for this task are the "Partial Glide Method" and the "Glider Comparison Method" ([1],[5],[6]) completed lately by the "Speed Reduction Method" ([8]). All of them need special flight tests.

### Partial Glide Method:

One performs stationary, straight flights in very calm air at certain air speeds; the altitude differences and the affiliated flight periods yield the sink rates. Because one needs several flights, this method is very time-consuming.

### Glider Comparison Method:

One needs a reference glider measured by the Partial Glide Method. Together with the sailplane under investigation one performs stationary, straight formation flights; the relative altitude differences at the beginning and at the end as well as the flight periods yield the sinkrate differences between the two gliders; and hence

the new polar by means of that of the reference plane. The number of necessary flights is smaller than the one of the Partial Glide Method.

### Speed Reduction Method:

During an instationary, straight flight of about 120 s in calm air one covers the whole range of the polar from maximum to minimum air speed. The number of necessary flights is again relatively small.

All three methods treat the influence factors 2. and 3. of subsection 1.1 in a similar manner: for  $C_L$  and  $C_D$  one gets information which is only applicable to the individual glider under investigation, as measuring many sailplanes of one type is not practical. The following new method determining the polar would be more universal:

- usable during normal soaring flight, not only in flight tests,
- short measurement periods,
- no influence on the sailplane,
- moderate need for measuring equipment,
- good polar recording at low air speeds.

That means the determination of the individual, time varying speed polar. We assume no special flight manoeuvres and wind conditions; so we have to investigate the instationary, straight flight and to estimate the wind vector in real-time.

## 2 System Model

### 2.1 Identification Task

The sailplane and its measuring devices constitute a system. To ascertain those system properties which determine the polar, we use the term "identification".

Figure 4 shows the identification strategy: A certain input signal excites the sailplane; and the subsequent measuring instruments indicate the corresponding reactions; the same input acts on a mathematical model which copies the system of the glider and the measuring devices, including the input signal a comparison of the model output with the measurement signals of the real system is the next step; the identification has to determine that special model which yields on this occasion to the best agreement for the output signals.

For example [9]-[13] deal with special aspects of ap-

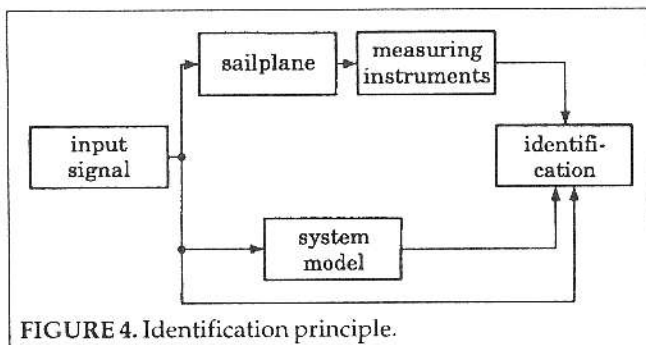


FIGURE 4. Identification principle.

plying the identification to tasks of flight mechanics, of modelling, and of choosing suitable algorithms. It follows from these informations that one can use the

Kalman-Filter and the Least-Square method, as we do in section 3.

### 2.2 Model Equations

Only  $C_L(\alpha)$  and  $C_D(\alpha)$  actually determine the polar; so we must just ascertain these two functions. But both coefficients act on the motion of the glider by the aerodynamic forces; therefore we need a dynamic system model.

It is advisable to use model equations consisting of two halves. The first one contains a system of differential equations which describe the time behaviour of the model; and the second one gives information about the measurement values and errors. The most important parts of the equations are the input signal, the state variable vector  $x$ , the measurement vector  $y$ , and the parameter vector  $c$ . One can find more details about the used model in [11].

### 2.3 State Variables

We need the state variables, because they represent the time behaviour of the system; this comprises the instationary, straight flight of a sailplane as well as wind and air properties being the surroundings. Therefore  $x$  consists of:

$$x = \begin{bmatrix} \text{flight-path velocity } VK \\ \text{flight-path inclination angle } \gamma \\ VW\text{-component parallel to } VK \\ VW\text{-Component perpendicular to } VK \\ \text{temperature } T \\ \text{static pressure } p \end{bmatrix}$$

The mentioned differential equations contain the changes of  $x$  with respect to time. The reason for the dynamical character of  $VK$  and  $\gamma$  is the acceleration by the aerodynamic forces of  $C_L$  and  $C_D$ .  $VW$  and  $T$  are not constant, because the glider moves through a wind and a temperature field, which vary spatially and by chance; to describe these accidental phenomena, one can use spectral densities and differential relations ([15]-[17]). In addition, the combination of the vertical temperature gradient with changing altitudes has an effect on  $T$ ; and the vertical pressure gradient ([18]) accordingly acts on  $p$ .

### 2.4 Measurement Values

The following aspects are essential for the choice of the measurement values ([6],[19]):

- use of well-established sensors and devices for the development of a new identification procedure;
- the measurement values must contain informations of all state variables; this is necessary for the Kalman-Filter;
- acceptable costs.

The measurement values are:

$$y = \begin{bmatrix} \text{static pressure} \\ \text{dynamic pressure} \\ \text{temperature} \\ \text{plane inclination} \\ \text{angle angle of attack } \alpha \end{bmatrix}$$

Measuring  $\alpha$  is a problem, but we need the time behaviour of the input signal. The estimation of the wind velocity requires in addition the plane inclination angle ([14]); because of acceptable costs other inertial sensor signals were temporarily disregarded. (Remark in anticipation of section 4: First tests of the described identification procedure revealed that an use of the Global-Positioning-System GPS is not helpful, because the accuracies and sampling rates of customary sets were not high enough.)

### 2.5 Aerodynamic Coefficients

The flow field around a sailplane is too complicated to allow an exact mathematical description of  $C_L$  and  $C_D$ . But approximations are sufficient for our given task, as the dashed curve of Figure 5 shows: this line can reproduce for instance the exact polar of the type ASW-19 ([2]), which was chosen by chance, if one uses the following polynomial series (compare also [20]):

$$C_L(\alpha) = C_{L0} + C_{L1}\alpha + C_{L2}\alpha^2 + C_{L3}\alpha^3 + C_{L4}\alpha^4 \quad (5)$$

$$C_D(\alpha) = C_{D0} + C_{D1}\alpha + C_{D2}\alpha^2 + C_{D3}\alpha^3 + C_{D4}\alpha^4 \quad (6)$$

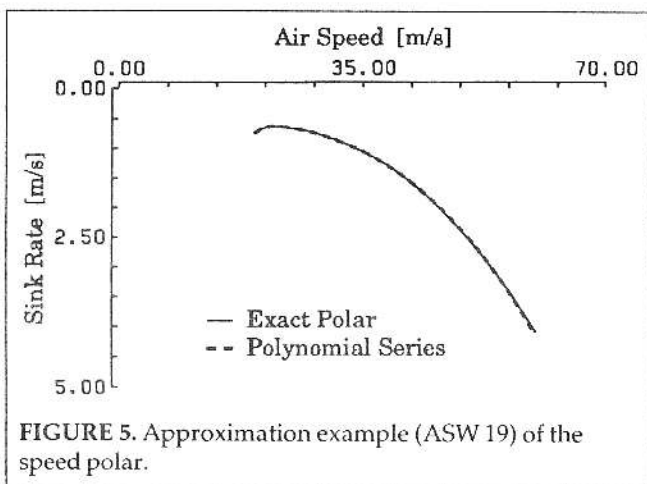


FIGURE 5. Approximation example (ASW 19) of the speed polar.

Except  $\alpha$ , the right sides of these equations only contain parameters, which are not available if the coefficient functions are unknown. But to get the speed polar, it is the task of the identification to determine  $C_L(\alpha)$  and  $C_D(\alpha)$ ; that means to estimate  $C_{L0}$  +  $C_{D4}$ . For this purpose we unite those symbols in the mentioned vector  $c$ :

$$c = [C_{L0}, C_{L1}, C_{L2}, C_{L3}, C_{L4}, C_{D0}, C_{D1}, C_{D2}, C_{D3}, C_{D4}]^T \quad (7)$$

### 3 Identification Procedure

Considering the three elements  $x$ ,  $y$ ,  $c$  leads us to the basic structure of the identification procedure, which consists of two parts explained in the subsections :3.2 and 3.3.

#### 3.1 Basic Structure

To gain the values of  $y$  is the task of the measurement devices; but at first the state variables  $x$  and the param-

eters  $c$  remain unknown. For this typical feature of identification in flight mechanics procedures consisting of two steps are usual ([21]-[23]): one determines first the time behaviour of  $x$ ; and afterwards one calculates  $c$ . Figure 6 shows the process (its realization should be carried out by means of a digital computer); we combine the two methods mentioned at the end of subsection 2.1:

1st step **flight reconstruction**: Kalman-Filter, Estimation:  $y \rightarrow x$ ;

2nd step **parameter-identification**: Least-Square, Estimation:  $x \rightarrow c$ .

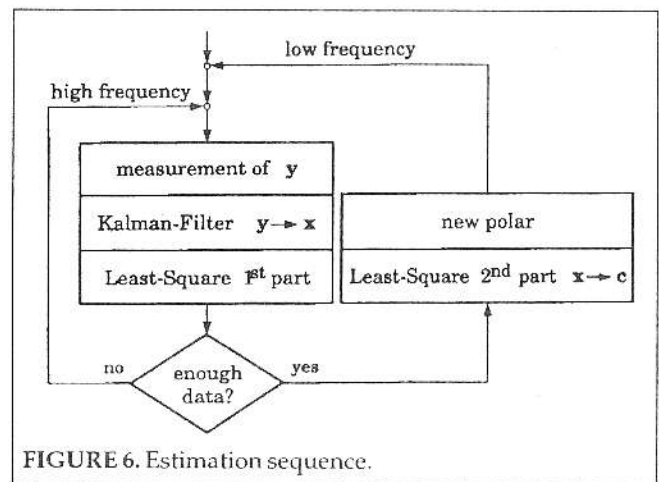


FIGURE 6. Estimation sequence.

When enough data are gathered, one can calculate the unknown parameters and determine the polar. Because some influence factors of the standardized polar are not constant,  $c$  changes slowly; but the repetition of the  $c$ -estimation with a low frequency facilitates following those variations. (For details see [14].)

#### 3.2 Kalman-Filter

The Kalman-Filter estimates the effects of accidental disturbances like gusts and model inaccuracies; it calculates the statistically most probable  $x$ -values. For this task it needs parameters, which are unknown at first; initially we use theoretical data. [16],[24] and [25] contain the filter equations as well as related problems; here one should only mention three aspects:

- nonlinear model equations (reason: equations of flight mechanics),
- $x$  continuous in time,  $y$  discrete in time (reason: digital computer),
- low computational amount (reason: real-time processing).

One can test the suitability of the corresponding formulas if accurate simulation results are available (which serve as measurement data for the Kalman-Filter and as a basis of comparison). Figure 7 shows an example (from [14]); it contains the accelerations parallel and perpendicular to the path during a straight flight of a glider in

turbulent air. The estimated, dotted lines agree sufficiently with the exact curves.

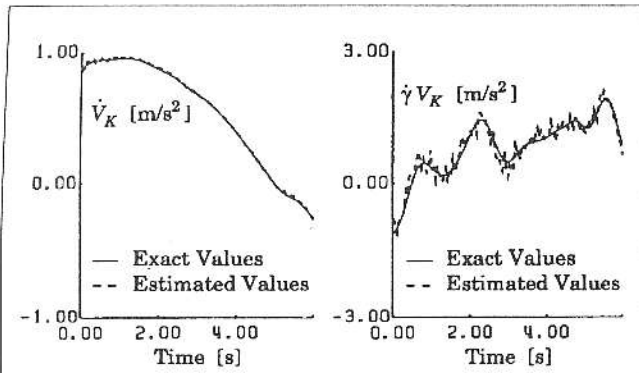


FIGURE 7. Estimation example for the flight-path acceleration.

### 3.3 Least-Square

The Least-Square method has to determine the values of the parameters. Figure 8 illustrates the estimation principle with the example of  $C_L$ ; the points are from the Kalman-Filter results and the solid line represents the polynomial of equation (5) which has the minimal mean distance from them. The parameters of  $C_D$  follow accordingly.

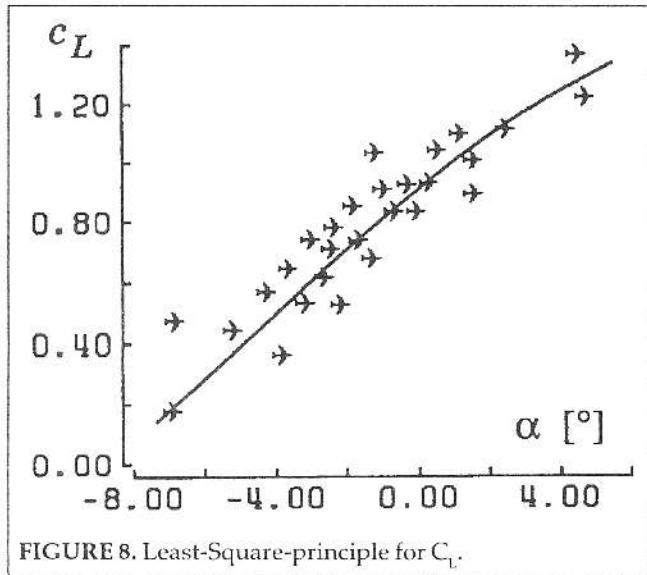


FIGURE 8. Least-Square-principle for  $C_L$ .

First, the high sampling rate of the Kalman-Filter produces a large amount of data; this is necessary to get reliable Least-Square estimations; if one processes the series of numerical values by a recursive way, an extensive, temporary data storage can be dropped. Secondly, high and low angles of attack occur relatively seldom; so the  $C_L$ - and  $C_D$ -points have an uneven arrangement over the interesting  $\alpha$ -interval; this is a problem for a regular approximation of the polar, which needs a fairly even distribution; but one can reach such conditions if one uses repeatedly the data points of the weakly occu-

ried  $\alpha$ -ranges to give them a higher weight ([26]).

## 4 Results and Conclusions

One can use the mentioned simulation data to check not only the Kalman-Filter but also the whole procedure. This method of testing has two advantages: it is easy to distort the artificial measurement signals by additional errors; and one knows the exact polar in advance. In the following results the Kalman-Filter had a sampling rate of 100 Hz and the Least-Square estimation gathered data over a period of 135 s.

Figure 9 shows standardized polars for the ASW 19. The line of those parameters for the Kalman-Filter was determined before the test and the exact curve coincide; also the polar calculated after the first Least-Square estimation agrees with these even if the measurement values contain additional noise; but worse results arise for the case of further, artificial measurement biases (which had the order of about 2% of the necessary measurement ranges). So the presented method needs carefully calibrated sensors.

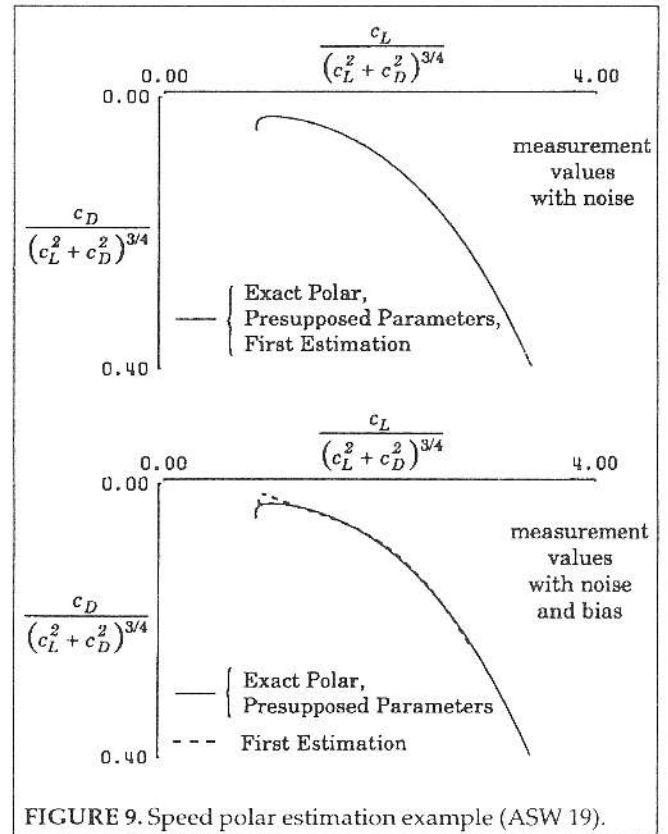


FIGURE 9. Speed polar estimation example (ASW 19).

The results show the suitability of the chosen method. One can also see the next problem: determining systematically the influence of sensor errors; considering the convergence behaviour if the parameter of the Kalman Filter calculated in advance are inaccurate; examining the question whether polynomial series of lower order are sufficient for  $C_L$  and  $C_D$ ; and analyzing measurement data from real flight tests.

### Symbols

$c$	matrix of the parameters for $C_L$ and $C_D$
$C_D$	total drag coefficient
$C_{D0}+C_{D4}$	parameters for $C_D$
$C_L$	total lift coefficient
$C_{L0}+C_{L4}$	parameters for $C_L$
$D$	total drag
$L$	total lift
$mg$	sailplane weight
$p$	static pressure
$S$	wing area
$T$	temperature
$u_g$	horizontal component of $V$ (normal earth-fixed axis system)
$u_{Kg}$	horizontal component of $V_K$ (normal earth-fixed axis system)
$V$	air speed
$V_K$	flight-path velocity (absolute)
$V_W$	wind velocity (absolute)
$w_g$	vertical component of $V$ (normal earth-fixed axis system)
$w_{Kg}$	vertical component of $V_K$ (normal earth-fixed axis system)
$x$	matrix of the system state variables
$y$	matrix of the measurement values
$\alpha$	angle of attack
$\gamma$	flight-path inclination angle
$\rho$	air density
$opt$	mark for an optimum
*	mark for a standardization

### References

- [1] Thomas, F., 1984, *Grundlagen für den Entwurf von Segelflugzeugen*. 2. Aufl. Stuttgart: Motorbuch.
- [2] Laurson, H., Zacher, H., 1977 Flugmessungen an 35 Segelflugzeugen und Motorseglern. Teil I bis IV. *Aerokurier* 1977.
- [3] Stich, G.; Treiber, H., 1981 Die Berechnung der Widerstandspolaren von Segelflugzeugen. *Arbeitsbericht DFVLR FF-FM BS / Schempp-Hirth KG*, not published.
- [4] Lammlein, S.T.; Ewald, B., 1988 Berechnung der Geschwindigkeitspolaren von Segelflugzeugen unter Berücksichtigung von Nichtlinearitäten. *Jahrbuch 1988 I der DGLR*, pp. 597-602.
- [5] Laurson, H.; Schmerwitz, D., 1987 Entwicklung der Polarenmessung. Aachen: Idaflieg (1937-1987).
- [6] Schmerwitz, D., 1988 Sailplane Performance Flight Test Techniques of DFVLR. Lecture, *SSA Convention, Atlanta/Georgia: 1988*.
- [7] Krauspe, P., 1983 *Beiträge zur Längsbewegung von Flugzeugen in Windscherungen*. Diss. TU Braunschweig.
- [8] Albat, A., 1992 *Untersuchung der Ausschießmethode mit veränderlichem Bahnwinkel für die Flugleistungsvermessung von Segelflugzeugen*. IB 111-92/31, Institut für Flugmechanik, DLR Braunschweig.
- [9] Hamel, P.G., 1987 Flight Vehicle System Identification - Status and Prospects. *DFVLR-Mitt.* 87-22, pp. 52-90.
- [10] Isermann, R., 1988 *Identifikation dynamischer Systeme*. Band I/II. Berlin, Heidelberg, ...: Springer.
- [11] Klein, V., 1979 Identification Evaluation Methods. AGARD-LS-104, No. 2.
- [12] Schanzer, G., 1990 Modelling of Aerospace Systems. Preprints of the *Second Braunschweig Aerospace Symposium: Real-Time Models for Control, Measurement, and Estimation Systems*, pp. 27-41.
- [13] Tischler, M.B.; Kaletka, J., 1987 Modeling XV-15 Tilt-Rotor Aircraft Dynamics by Frequency and Time-Domain Identification Techniques. AGARD-CP-423, No. 9.
- [14] Wagner, J., 1992 *Zur Simulation und Identifikation der Segelflug-Längsbewegung*. Submitted dissertation, Universität Stuttgart, Fakultät Verfahrenstechnik.
- [15] Houbolt, J.C., 1973 Atmospheric Turbulence. *AIAA J.* 11, pp. 421-437.
- [16] Da, R.; Brockhaus, R., 1989 Untersuchung eines nichtlinearen Kalman-Filters zur Schätzung von Zustandsgrößen eines Flugzeugs. *ZVW* 13, pp. 326-333.
- [17] Stull, R.B., 1988 *An Introduction to Boundary Layer Meteorology*. Dordrecht, Boston, London: Kluwer Academic Publishers.
- [18] 1979 *DIN-ISO 2533 Normatmosphäre*. Berlin, Köln: Beuth.
- [19] Breemann, J.H., et al. 1979 Aspects of Flight Test Instrumentation. AGARD-LS-104, No. 4.
- [20] Kloster, M., 1977 *Flugleistungen mit exponentiellen Widerstandspolaren*. Diss. TU München.
- [21] Parameswaran, V.; Plaetschke, E., 1990 Flight Path Reconstruction Using Extended Kalman Filtering Techniques. *DLR-FB 90-11*.
- [22] Proskawetz, K.O. 1991 System-Identification of Airplanes Using the "Estimation Before Modelling" Technique. *ZFW* 15, pp. 401-407.
- [23] Wang, W.; et al., 1989 Flugversuchsdaten-Korrektur durch Flugbahnrekonstruktion mit einem nichtlinearen Sechs-Freiheitsgrade-Modell. at 37, pp. 226-233/258-263.
- [24] Gelb, A. (ed.), 1974 *Applied Optimal Estimation*. Cambridge, Massachusetts, London: The M.I.T. Press.
- [25] Krebs, V., 1980 *Nichtlineare Filterung*. München, Wien: R. Oldenbourg.
- [26] Haverland, M., 1988 Ein lernender Regler für die Flugzeuglängsbewegung. Diss. TU Braunschweig.